Remote Sensing of Environment 122 (2012) 41–49

Contents lists available at SciVerse ScienceDirect

Remote Sensing of Environment

journal homepage: www.elsevier.com/locate/rse

Thermal infrared radiometric calibration of the entire Landsat 4, 5, and 7 archive (1982–2010)

John R. Schott [a,*], Simon J. Hook [b], Julia A. Barsi [c], Brian L. Markham [d], Jonathan Miller [e], Francis P. Padula [f], Nina G. Raqueno [a]

[a] Rochester Institute of Technology, United States
[b] Jet Propulsion Lab, California Institute of Technology, NASA, United States
[c] Science Systems and Applications, Inc., NASA, United States
[d] GFSC, NASA, United States
[e] USAF, United States
[f] Science Applications International Corporation, United States

ARTICLE INFO

Article history:
Received 11 March 2011
Received in revised form 20 June 2011
Accepted 18 July 2011
Available online 17 February 2012

Keywords:
Infrared
Radiometric calibration
Landsat
Residual uncertainty

ABSTRACT

Landsat's continuing record of the thermal state of the earth's surface represents the only long term (1982 to the present) global record with spatial scales appropriate for human scale studies (i.e., tens of meters). Temperature drives many of the physical and biological processes that impact the global and local environment. As our knowledge of, and interest in, the role of temperature on these processes have grown, the value of Landsat data to monitor trends and process has also grown. The value of the Landsat thermal data archive will continue to grow as we develop more effective ways to study the long term processes and trends affecting the planet. However, in order to take proper advantage of the thermal data, we need to be able to convert the data to surface temperatures. A critical step in this process is to have the entire archive completely and consistently calibrated into absolute radiance so that it can be atmospherically compensated to surface leaving radiance and then to surface radiometric temperature. This paper addresses the methods and procedures that have been used to perform the radiometric calibration of the earliest sizable thermal data set in the archive (Landsat 4 data). The completion of this effort along with the updated calibration of the earlier (1985–1999) Landsat 5 data, also reported here, concludes a comprehensive calibration of the Landsat thermal archive of data from 1982 to the present.

© 2012 Elsevier Inc. All rights reserved.

1. Introduction and summary

Landsat's continuing record of the thermal state of the earth's surface represents the only long term (1982 to the present) global record with spatial scales appropriate for human scale studies (i.e., tens of meters). Note, AVHRR data span from 1978 to the present and Modis data span from 2000 to the present with 1 km pixels. Temperature drives many of the physical and biological processes that impact the global and local environment. As our knowledge of, and interest in, the role of temperature on these processes has grown, the value of Landsat data to monitor trends and process has also grown. Areas of study that use Landsat derived thermal data include lake hydrodynamic process (Schott, 1986; Schott et al., 2001), monitoring evapotranspiration (Allen et al., 2008; Anderson & Kustas, 2008), regional water resources (Thenkabail et al., 2009, 2010), and the impact of local climate trends (Schneider et al., 2009). The value of the Landsat thermal data archive will continue to grow as we develop more effective ways to study the long term processes and trends affecting the planet. However, in order to take proper advantage of the thermal data, we need to be able to convert the data to surface temperatures. A critical step in this process is to have the entire archive completely and consistently calibrated into absolute radiance so that it can be atmospherically compensated to surface leaving radiance and then to temperature. This paper addresses the methods and procedures that have been used to perform the radiometric calibration of the earliest sizable thermal data set in the archive (Landsat 4 data). The completion of this effort along with the updated calibration of the earlier (1985–1999) Landsat 5 data, also reported here, concludes a comprehensive calibration of the Landsat thermal archive of data from 1982 to the present. The different methodologies used to accomplish the entire calibration/validation update are reviewed in Section 2. The new results for Landsat 4 and early Landsat 5 as well as the previously reported results for Landsats 5 and 7 (Barsi et al., 2003; Hook et al., 2004) are included in Section 3. In particular, this section includes a discussion of the small residual uncertainty in the data archive associated with each data set. This uncertainty in the collective archive

* Corresponding author. Tel.: +1 585 475 5170; fax: +1 585 475 5988.
E-mail address: schott@cis.rit.edu (J.R. Schott).

0034-4257/$ – see front matter © 2012 Elsevier Inc. All rights reserved.
doi:10.1016/j.rse.2011.07.022

of approximately 0.6 K means that, with good knowledge of the atmosphere and emissivity, surface temperatures can be retrieved to better than 0.7 K (one sigma) using standard analytical approaches. These results mean that for the first time users can access and analyze the entire 30 year record with confidence in the radiometric integrity of the thermal data.

2. Background

This section will introduce the Landsat sensors from the thermal infrared perspective and then briefly review the approaches that have been used over time for vicarious radiometric calibration of the Landsat thermal instruments.

2.1. Instruments

Landsat 3 was the first Landsat satellite to include a thermal sensing capability. However, the thermal sensor failed quite early in the mission and no significant effort has yet been expended to characterize its post launch performance. Therefore, this paper will focus on the thermal sensors on the Landsat 4 Thematic Mapper (TM4), the Landsat 5 Thematic Mapper (TM5) and the Landsat 7 Enhanced Thematic Mapper plus (ETM+). From the thermal infrared perspective these three instruments were nearly identical with the exception being that ETM+ had eight thermal detectors instead of the 4 on the TM instruments resulting in a 60 m ground instantaneous field of view (GIFOV) instead of 120 m for the TM instruments. Each instrument had a single spectral band nominally covering the 10.5–12.5 μm spectral window (see Fig. 1) with two eight bit gain settings. Fig. 2 shows a generic optomechanical schematic of the instruments highlighting the elements relevant to the thermal band. In particular, note that on the TM instrument 4 detectors are swept across the field of view (FOV) forming 4 120 m lines of data per sweep of the scan mirror and that on ETM+ 8 detectors sweep 8 60 m lines of data. Also note that as the scan mirror is turning around, a calibration shutter is inserted into the line of sight. The shutter has a high emissivity surface with a monitored temperature and a mirror that reflects a cavity blackbody into the line of sight. Thus, as the shutter is swept into the line of sight, the detectors "see" first the known radiance from the shutter and then the known radiance from the blackbody. This provides a two point calibration at the beginning and end of each line of data. These two points are used to calculate the internal gain (g_i) according to

$$g_i = \frac{DN_{BB} - DN_S}{\hat{L}_{BB\lambda} - \hat{L}_{S\lambda}} \tag{1}$$

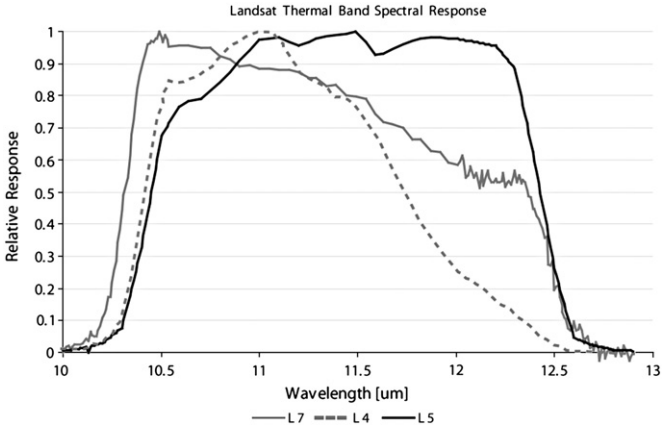

Fig. 1. Plots of the relative spectral response of the TM4, TM5 and ETM+ instruments.

where DN_{BB} and DN_S are the average digital number from a sample of image data taken from the blackbody and the shutter respectively and $\hat{L}_{BB\lambda}$ and $\hat{L}_{S\lambda}$ are the spectral radiance in the passband associated with a blackbody at the temperature of the blackbody (BB) and shutter (S) respectively, i.e.

$$\hat{L}_{BB\lambda} = \frac{\int L_{BB\lambda} R(\lambda) d\lambda}{\int R(\lambda) d\lambda} \tag{2}$$

where $L_{BB\lambda}$ is the spectral radiance from a blackbody at temperature BB [W m^{-2} sr^{-1} μm^{-1}] and $R(\lambda)$ is the relative spectral response of the sensor with wavelength λ.

The actual sensor output (DN) can then be related to the radiance from the scene (L_λ) as

$$DN = g_f(g_i L_\lambda + b_i) + b_f \tag{3}$$

where b_i is an internal bias level related to the shutter radiance (i.e. shutter temperature) and g_f and b_f are gain and bias terms associated with multiplicative and additive effects not captured by the internal calibration process (e.g. transmission losses from the optics forward of the shutter and additive radiance from the optics forward of the shutter). Note that the actual equations used in the software for the different instruments vary slightly from instrument to instrument but can be generalized to the form shown in Eq. (3).

Values for the remaining calibration coefficients (i.e. b_i, g_f and b_f in this representation) were determined from pre-launch laboratory calibration with external radiance sources. Given these calibration coefficients, the sensor reaching radiance can be calculated from the recorded DN for each pixel by inversion of Eq. (3). Some of these coefficients are dependent on the operating temperatures of the forward optics. In practice, coefficients appropriate for the expected operating temperatures were calculated empirically pre-launch, however, no trusted fore-optic calibration model was developed which would allow adjustment of the coefficients based on the recorded temperatures of the optical elements. Thus, when significant changes to the instrument's operating temperatures occur (either planned or unplanned), or if there is degradation of the forward optics, new values for the calibration coefficients must be determined and applied to the calibration equation (Eq. 3) to maintain the calibration of the data. Because there is no onboard system to adequately monitor any radiometric changes in the forward optics, vicarious calibration procedures have been regularly used to verify the stability of the calibration after launch and then (at least since 1999) to monitor the calibration on orbit.

2.2. Vicarious calibration approaches

Four different vicarious calibration techniques have been used to support the calibration of the Landsat thermal bands. Each of these will be introduced in this section. All of the methods use water as a target. Water is an ideal target because of its high thermal inertia, high emissivity and as a liquid it is hard to maintain thermal gradients, so large regions of uniform temperature are common (Schott et al., 2004; Tonoka et al., 2005). All of the methods also use the radiation propagation code MODTRAN (Berk et al., 1999) to propagate the radiation to the sensor. The governing radiometry equations and the use of MODTRAN will therefore be introduced in Section 2.2.1 before the discussion of the different measurement techniques.

2.2.1. Atmospheric propagation

The governing equation for radiation propagation to the sensor can be expressed as

$$\hat{L}_\lambda = \frac{\int [(\varepsilon(\lambda) L_{T\lambda} + (1-\varepsilon(\lambda)) L_{d\lambda}) \tau(\lambda) + L_{u\lambda}] R(\lambda) d\lambda}{\int R(\lambda) d\lambda} \cong \hat{L}_{obs\lambda} \tau + \hat{L}_{u\lambda} \tag{4}$$

Download English Version:

https://daneshyari.com/en/article/4459142

Download Persian Version:

https://daneshyari.com/article/4459142

Daneshyari.com